

Plasmochromic Modules for Smart Windows: Design, Manufacturing and Solar Control Strategies

Mirco Riganti¹, Julia Olive¹, Francesco Isaia², Michele Manca¹

* Corresponding author, mmanca@leitat.org

1 LEITAT Technological Center, Terrassa, Barcelona, Spain

2 Eurac research, Institute for Renewable Energy, Energy Efficiency Buildings – Building envelope technologies, Bolzano, Italy

Abstract

Active glazing components, which can dynamically regulate incoming solar radiation, are particularly interesting, as they simultaneously impact multiple aspects, such as thermal and visual comfort and overall energy consumption. Near-infrared EC windows (also referred to as “plasmochromic”) enable selective spectral control of the incoming solar radiation and efficiently respond to ever-changing lighting, heating and cooling requirements. They allow to selectively filter a large amount of near-infrared solar radiation passing through the window, thus blocking solar heat gain during hot summer days and letting it permeate over sunny winter days whilst independently regulating the amount of daylight. This article delves into the core attributes of such glazing systems, showcasing recent advancements in their design and fabrication. By evaluating key metrics like luminous transmittance (T_{LUM}), solar transmittance (T_{SOL}), and total solar heat gain coefficient (g-value), the paper presents a preliminary performance assessment of smart glazing employing this technology. Furthermore, the authors prospect the importance of implementing appropriate control strategies for these systems to fully exploit their potential in reducing energy consumption while maximising comfort.

Keywords

solar control, EC windows, plasmochromic devices, energy efficient glazing

DOI

<http://doi.org/10.47982/jfde.2023.2.T3>

1 INTRODUCTION

The building sector, accounting for approximately 20% of global primary energy consumption, is projected to see significant growth due to population increase and rising living standards (Cao, Dai, & Liu, 2016). The energy requirements for heating, cooling, and lighting are primary contributors to this consumption. Smart glazing systems have emerged as a pivotal technology to enhance energy efficiency and cost savings.

The “window of the future” is envisioned to transition from a vulnerable point in building design to a multifunctional unit with adaptable properties. These windows should seamlessly integrate into a building’s climate control and lighting systems (Favoino & Overend, 2015). Active glazing components, which can modulate solar radiation, are especially appealing. However, current EC windows cannot selectively filter thermal radiation without impacting luminous transmittance.

In contrast, “plasmochromic” (PLSMC) devices, using transparent plasmonic semiconducting nanocrystals as active EC layers, offer a solution to these limitations (Li, Niklasso, & Granqvist, 2012). These materials, allowing for fine-tuning their optical properties, have been developed and implemented by various research groups (Cao, Zhang, Zhang, & Lee, 2018; Garcia et al., 2011; Tsuboi, Nakamura, & Kobayashi, 2016; Xu et al., 2018). This technology enables the creation of intelligent building skins that can dynamically adjust to external and internal conditions, integrating with an “Internet of Things” (IoT) platform for optimised control.

Our recent research has unveiled the unique solar control features of these systems in the near-infrared (NIR) region that can, in principle, enable an independent modulation of the optical transmittance of a smart window in two distinct spectral ranges, namely VIS and NIR ranges (Barawi et al., 2018; Cots et al., 2021). A PLSMC glazing system, as illustrated in Fig. 1, is laminated on the interior side of the exterior glass. In its open circuit potential (OCP), or “warm state”, the device allows both VIS and NIR radiation into the building. When a low/moderate negative bias is applied, it selectively blocks NIR radiation while maintaining VIS transparency, referred to as the “cold state.” At higher negative potentials, incoming radiation is filtered across the solar spectrum, creating a “dark state” that combines full NIR radiation extinction with intense blue colouring.

The primary aim of this paper is to delve into the design, production, and implementation of plasmochromic modules in smart windows. The article also strives to assess the advanced solar control capabilities these modules offer and to present an analysis of control strategies to optimise their performance. Finally, through comparative analysis, the intention is to position plasmochromic modules against the backdrop of existing shading technologies, highlighting their distinctive advantages.

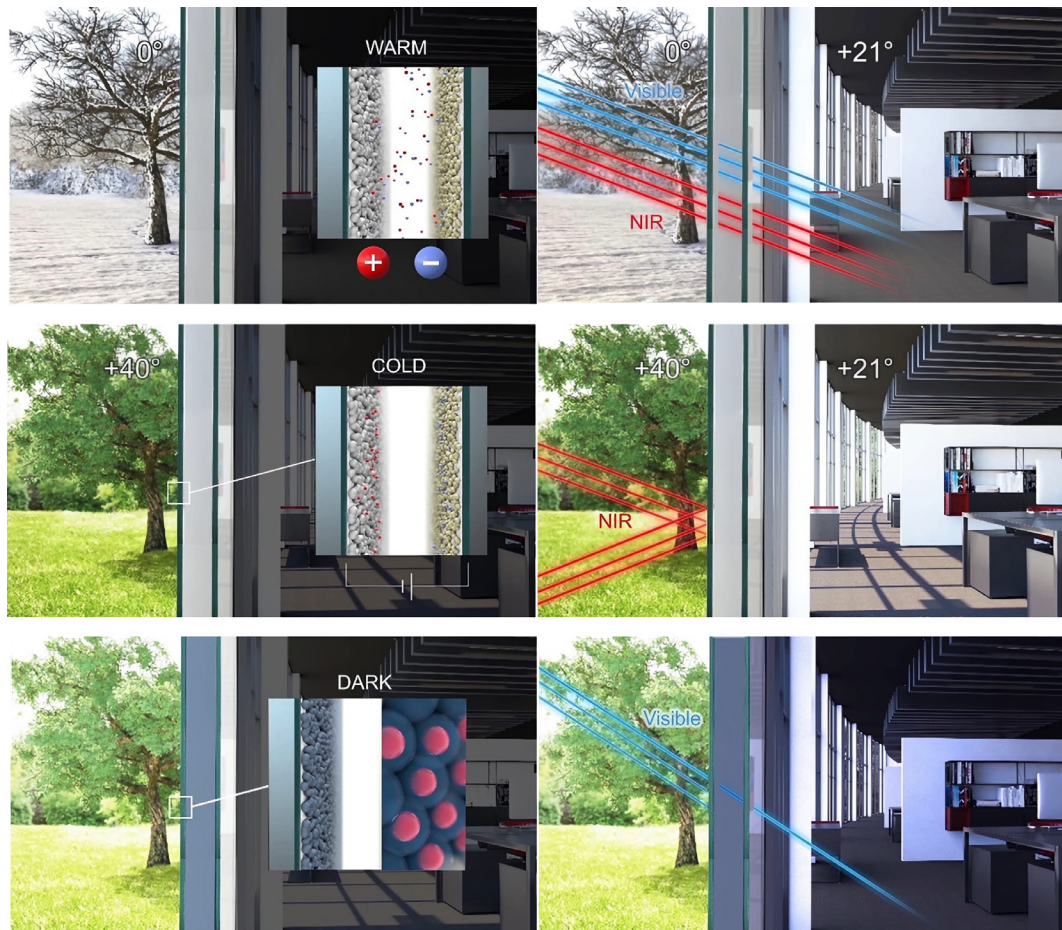


FIG. 1 Functioning schematic of a PLSMC glazing system. (a) In winter, the system allows NIR solar radiation to pass through, acting as a proactive heating mechanism. (b) During mid-season/summer, it can selectively filter out incoming thermal radiation in response to daily changes in sunlight orientation and intensity, blocking up to 95% of NIR radiation, thereby acting as a proactive cooling system. (c) The system also enables independent control of visible sunlight to reduce glare and ensure optimal visual comfort.

2 RESEARCH FRAMEWORK AND METHODOLOGY

This investigation focuses on the capabilities of near-infrared electrochromic or plasmochromic windows to dynamically control incoming solar radiation, emphasising their impact on thermal and visual comfort as well as energy consumption. Our research integrates a blend of experimental procedures with computational modelling to not only gauge the PLSMC modules' efficacy under diverse environmental stimuli but also to estimate their influence on the energy performance and internal environment of buildings.

The study unfolds across several methodically organised stages:

- 1 Design and Prototyping:
 - a Development of PLSMC modules initiated with the formulation of specialised inks conducive to a scalable roll-to-roll manufacturing process, optimising aspects such as viscosity and environmental impact of solvents and additives.
 - b Prototypes were then crafted, integrating nanostructured coatings into glazing units while ensuring compatibility with large-scale production and end-use applications.
- 2 Characterisation and Performance Analysis:
 - a Detailed assessment of the optical and thermal properties of the PLSMC modules, examining their performance spectrum across various activation states.
 - b The modules underwent rigorous testing to ascertain key performance metrics, including solar transmittance and luminous transmittance.
- 3 Computational Simulation and Control Strategy Development:
 - a Empirical data from the initial phases were translated into simulation models to predict the behaviour of buildings outfitted with PLSMC smart windows.
 - b Investigation into advanced control algorithms, including Rule-Based Control (RBC) strategies, aimed to optimise the automatic regulation of smart EC glazing systems.
- 4 Integration and Evaluation in Building Context:
 - a Synthesis of the experimental and simulation data facilitated the exploration of PLSMC modules within the context of building integration, considering factors like solar load modulation and visible light transmission.
 - b Comparative analyses were conducted to juxtapose the performance of PLSMC technologies against conventional glazing systems, underscoring the advantages of PLSMC in energy efficiency and occupant comfort.

2.1 PLSMC MODULE DEVELOPMENT AND PROTOTYPING

A pivotal issue in the viable industrialisation of this technology consists in the implementation of an “easily-up-scalable” manufacturing process based on roll-to-roll deposition of engineered PLSMC inks. Formulation of the inks includes optimisation of the viscosity, concentration, and environmental impact of solvents and additives. Another key aspect refers to the development of free-standing ion conductive membranes (namely free-standing electrolyte foils) suitable to be laminated at an industrial scale. In general, optimising the architecture and the fabrication procedure of PLSMC modules for large areas remains a major challenge.

PLSMC modules are based on the sandwich-like structure illustrated in Fig. 2. This structure comprises a transparent conductive oxide (TCO) deposited onto a first glass plate, an active PLSMC electrode, a solid ion conductor, a counter-electrode, and another layer of TCO deposited onto a second glass plate.

The manufacturing process consists of four crucial steps, some of which are shown in Fig. 3:

- 1 Ink deposition on transparent conductive glass through serigraphy methodology (both PLSMC and counter electrode inks). In-line drying at 180°C through IR radiation.
- 2 Thermal sintering of the as-deposited films at 450°C.
- 3 Gel electrolyte deposition.
- 4 PLSMC module lamination.

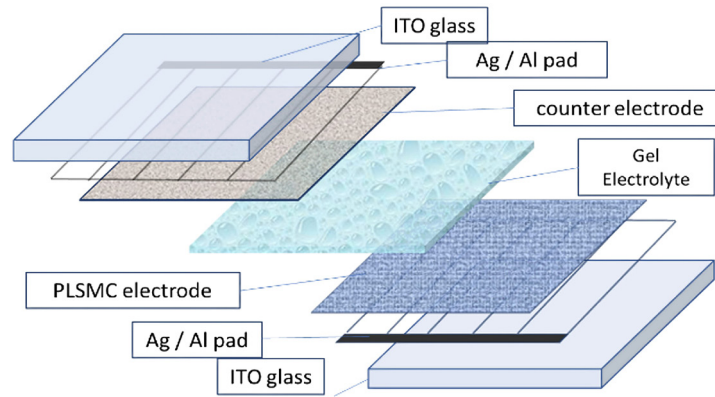


FIG. 2 Schematic illustration of the layers composing a PLSMC module.

Both active and passive nanostructured electrodes have been obtained by screen-printing (and subsequent thermal treatment) of viscous pastes containing engineered metal-oxide (plasmonic) nanocrystals. A configuration employing tungsten oxide and cerium oxide layers, interspersed by a lithium-ion electrolyte, has been implemented. Upon application of an external potential, lithium ions migrate towards the WO_x layer, inducing an alteration in its crystalline structure. This structural modification directly affects the material's optical properties, particularly its absorption spectra. Concurrently, the cerium oxide layer not only acts as a counter electrode, aiding in the ion migration process, but also contributes to the stability of the system. Importantly, the cerium oxide layer provides memory effects, ensuring the retention of distinct optical stationary states the device can adopt. Reversing the potential causes the lithium ions to depart from the WO_x matrix, returning the device to its original optical characteristics.

Modules of both 55x45 cm² and 70x130 cm² have been fabricated by using a semi-automated screen-printing machine (FIG. 3a) equipped with a stainless-steel screen mesh stretched under 20 N m⁻¹ tension in an aluminium frame. Screen-printed coatings, both the PLSMC active electrode and the counter electrode, have been dried for 15 minutes at 180°C in an IR oven and then subjected to thermal sintering in a ceramic furnace at 450°C with an optimised heating ramp-up. A set of sintered 45x55 cm² PLSMC films is shown in Fig. 3b.

The two coated glass palates were then assembled to form the PLSMC sandwich by laminating a UV-curable gel electrolyte cast onto one of two electrodes (Fig. 3b). The sandwich was exposed to UV radiation for 30 minutes (Fig. 3c) and then sealed at the edges with silicone resin that prevents moisture penetration. To reduce the ohmic resistance and improve the current distribution homogeneity, a copper current collector tape was attached to the edges of the TCO-glass panes.

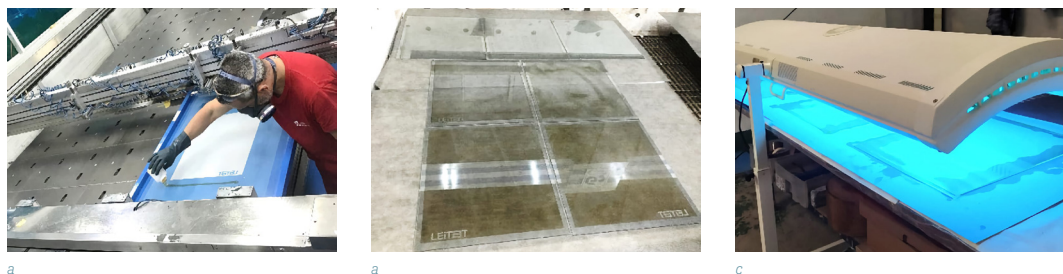


FIG. 3 (a) Semi-automated screen-printing machine. (b) Image of the PLSMC device assembled. (c) UV treatment of the prototype under a 365 nm wavelength light.

A 70x130 cm² PLSMC module is shown in Fig. 4, both in the bleached (WARM) and the coloured (DARK) state. Challenges have been identified in fabricating PLSMC modules exceeding dimensions of 70x130 cm². The primary concerns revolve around issues such as paste non-uniformity and inconsistencies in electrolyte deposition. Given that the technology is still in its developmental stages, with a current Technology Readiness Level (TRL) of 5, certain hurdles remain unaddressed.



FIG. 4 70x130 cm² PLSMC module respectively in the a) WARM and b) DARK state.

2.2 MODELLING OF A PLSMC IGU

The comprehensive performance evaluation of a glazing system heavily relies on the measurement of key parameters as well as the solar heat gain coefficient (g -value), the total visible transmittance (T_{LUM}), the total solar transmittance (T_{SOL}), and the thermal transmittance (U -value). These numbers have been obtained from the experimental transmittance and reflectance spectra of PLSMC devices, which have been properly processed with Optics (Optics, n.d.).

The insulating glass configuration selected for this study consists of a double-glazing unit (DGU) where the PLSMC module is laminated on the inner side of the exterior glass plate. Clear float glass has been chosen for both the exterior and interior glass to fully exploit the prerogatives of the PLSMC technology in the WARM state.

The thickness and type of the IGU typically depend on the application and associated insulating glass materials, which comprise metallic spacer, desiccant, sealants, laminating interlayer materials, and wiring. We have opted for a 31mm-thick IGU that embeds a low-emissive coating applied to the inner side of the interior glass and a 16 mm cavity filled with a mixture of argon (90%) and air (10%). See Fig. 5.

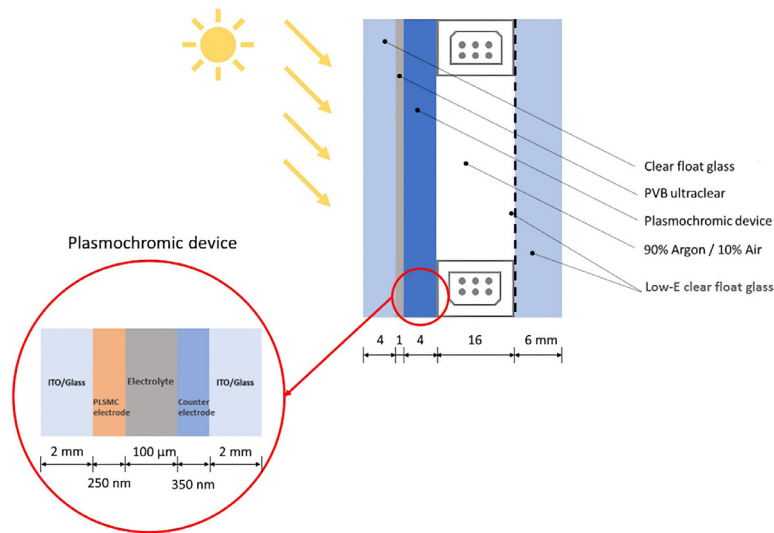


FIG. 5 Longitudinal section of a PLSMC DGU with a close-up section of the PLSMC device integrated in the DGU.

These properties have been calculated by means of the software tools Optics (Optics, n.d.) and WINDOW (WINDOW, n.d.) according to the formulas defined by ISO EN 410 (Standardization, ISO EN 410:1998. Glass in building. Determination of luminous and solar characteristics of glazing., 1998) and ISO EN 673 (Standardization, ISO EN 673:1997. Glass in building. Determination of thermal transmittance (U-value) - Calculation method., 2011):

$$T_{LUM} = \frac{\int_{380nm}^{780nm} D_{\lambda} V(\lambda) T(\lambda) d\lambda}{\int_{380nm}^{780nm} D_{\lambda} V(\lambda) d\lambda} \quad [-]$$

$$T_{SOL} = \frac{\int_{300nm}^{2500nm} I_{AM1.5,\lambda} T(\lambda) d\lambda}{\int_{300nm}^{2500nm} I_{AM1.5,\lambda} d\lambda} \quad [-]$$

$$g - \text{value} = T_{SOL} + q_i \quad [-]$$

$$U - \text{value} = \left(\frac{1}{h_e} + \sum R_i + \sum_{\lambda}^S + \frac{1}{h_i} \right)^{-1} \quad [W \cdot m^{-2} \cdot K^{-1}]$$

In formula (1), D denotes the relative spectral distribution of illuminant D65, $V(\lambda)$ is the spectral luminous efficiency for photopic vision, which defines the standard observer for photometry, and $T(\lambda)$ is the transmission value at a certain wavelength. λ represents the radiation wavelength in nm. In formula (2), $I_{AM1.5,\lambda}$ stands for the relative spectral distribution of solar radiation at 1.5 Air Mass. In formula (3), q_i represents secondary internal heat transfer towards the inside, accounting for the temperature difference between glass panes and the indoor environment. Formula (4) defines the U-value. Here, h_i and h_e are the internal and external surface heat transfer coefficients, respectively, R_i represents the thermal resistance of the i -layer, s refers to the thickness, and k denotes thermal conductivity.

To provide a realistic estimation of the most relevant thermal and optical properties of the PLSMC IGU, a set of commercially available glazing and shading solutions have been taken as benchmarks, namely:

- SageGlass SR2.0, an EC glass incorporated in a DGU with an internal low-E coating for dynamic control of light and heat transmission.
- Hella AR92S, a DGU with an internal low-E coating and an external blind, enabling flexible control over solar heat gain and light transmission.
- Pellini V95, triple glazing unit (TGU) featuring internal blinds and an internal low-E coating, offering superior thermal insulation and seamless control of light and privacy.

3 RULE-BASED CONTROL STRATEGIES FOR SMART GLAZING SYSTEMS

The potentialities of dynamic glazing with extended solar control properties are evident even to the most sceptical observers. However, the effectiveness of smart EC glazing systems strongly depends on their automatic regulation functionalities, underscoring the importance of adopting advanced control strategies to fully harness their potential.

Rule-Based Control (RBC) strategies are the most frequently utilised control algorithms for managing active glazing systems. These strategies are designed to trigger specific control actions when certain conditions are met. The most common driving variables used nowadays in RBC-based strategies include indoor temperature, outdoor temperature, solar radiation, illuminance, heating or cooling requirements, and occupancy levels.

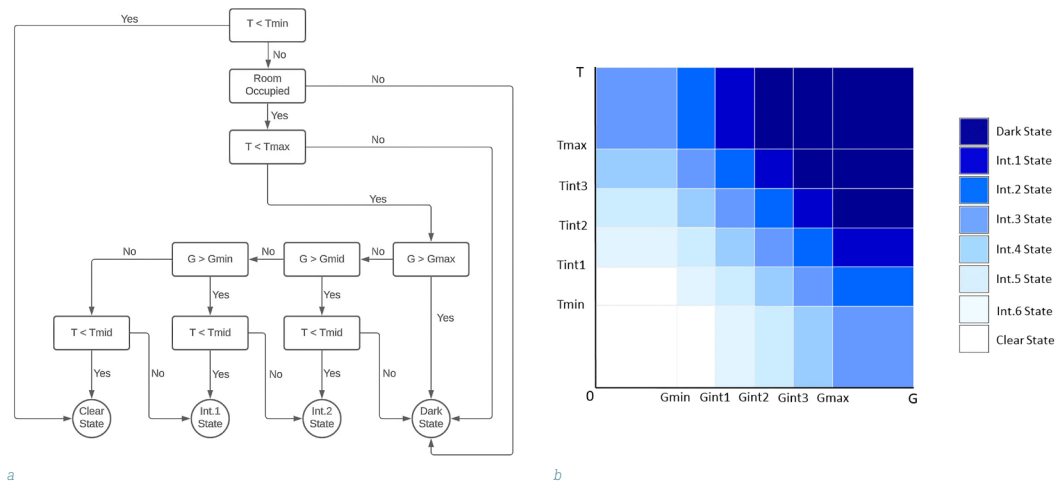


FIG. 6 (a) Flowchart of an RBC strategy based on internal air temperature (T) and incident solar irradiance on the window (G) made up of T_{min} , T_{mid} and T_{max} as indoor temperature thresholds, and G_{min} , G_{mid} , G_{max} as incident solar irradiance thresholds. (b) Cartesian representation of the same type of algorithm, using indoor temperature (T_{min} , T_{int1} , T_{int2} , T_{int3} , T_{max}) and incident solar irradiance (G_{min} , G_{int1} , G_{int2} , G_{int3} , G_{max}) thresholds.

An example of an RBC approach that may fit properly with the functional features of the PLSMC windows is depicted in the flowchart in Fig. 6a, which is based on the sequential consideration of three main variables: occupancy state, indoor temperature (T), and incident solar irradiance (G) (Roberts, De Michele, Pernigotto, Gasparella, & Avesani, 2022).

Based on the definition of n threshold values for indoor temperature T and incident solar irradiance G (in addition to the occupancy state), this algorithm can select and implement a number of discrete

states of the EC glazing to maximize both visual and thermal comfort. In Fig. 6b, the possible window's states are represented in the T vs G plane, where various regions are demarcated by the respective colour indicative of the EC state.

This control strategy may fit very well with the extended solar control prerogatives of PLSMC glazing, as its spectral selectivity would enable a finer balance between the (often competitive) needs for natural light and optimal indoor temperature. This key advantage of PLSMC systems with respect to "traditional" EC ones can be exploited with an advanced RBC algorithm capable of independently regulating T_{LUM} and the g-value. In Fig. 7, it is schematically represented as the combination of two 1-dimensional grids responding respectively to changes of G (horizontal tuning of T_{LUM}) and T (vertical tuning of g-value). As red gets more intense, the g-value of the PLSMC glazing gets lower (Fig. 7a). As blue gets more intense, T_{LUM} of the PLSMC glazing gets lower (Fig. 7b). The combination of two algorithms results in a comprehensive RBC strategy encompassing 36 distinct optical states (in comparison to the 8 states available with a "traditional" EC system) identified by a unique combination of T_{LUM} and g-value (see Fig. 7c).

This approach may, in principle, be able to account for seasonal variations in sunlight intensity and angle, as well as daily weather changes. For example, on a hot summer day with high solar irradiance, the system might trigger a state that reduces solar heat gain while maintaining adequate daylight. Conversely, on a cold but sunny winter day, it might allow for more solar heat gain while controlling the brightness levels.

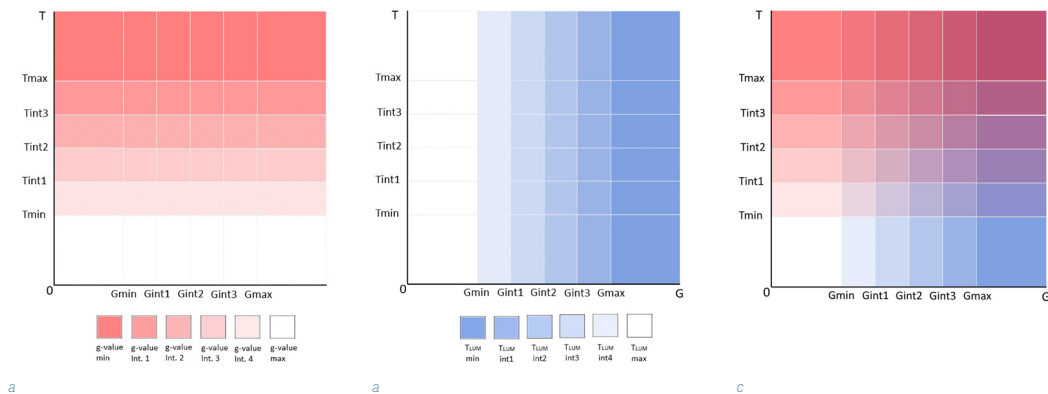


FIG. 7 (a) and (b) illustrate two complementary RBC algorithms optimized for PLSMC technology. The figures, using colour intensity scales, demonstrate how the algorithms modulate near Infrared and visible light transmittance based on varying indoor temperature and irradiance conditions. These algorithms use both the same indoor temperature (T_{min}, T_{int1}, T_{int2}, T_{int3}, T_{max}) and incident solar irradiance (G_{min}, G_{int1}, G_{int2}, G_{int3}, G_{max}) thresholds. In figure (c), the combination of the previous two algorithms led to a 36 states, with high thermal and visible modulation capability.

Nevertheless, the effects of incoming solar radiation on the indoor environment can be both immediate and long-lasting, as it heats the thermal mass and air within the space. Sophisticated control strategies can leverage these interconnected impacts, for instance, by adjusting solar gains in the short term to address immediate effects on occupant thermal and visual comfort while managing the building's thermal mass to optimise energy demand under comfort constraints. This aim can be realised by employing a control strategy that considers the building's thermal response to changes in input variables while effectively managing competing objectives. Among these strategies, Model Predictive Control (MPC) stands out for its capability to predict dynamic system response and calculate the optimal sequence of future inputs to minimize a specific cost function.

Isaia et al. have recently developed an innovative and efficient MPC (Isaia, Fiorentini, Serra, & Capozzoli, 2021), demonstrating its effectiveness in managing EC windows. This method successfully considers both continuous and discrete variables, resolving conflicting requirements and outperforming traditional rule-based controllers in key areas such as energy consumption, peak power, and discomfort hours.

An advanced MPC strategy may, in principle, further optimise the performances of PLSMC glazing. Depending on the priority, the controller can focus more on energy conservation or on maintaining indoor temperature for visual comfort, achieving a balance between these two objectives.

The performance of this MPC is largely determined by its specific configuration. For instance, prioritizing the heating/cooling system in the setup leads the controller to focus more on energy conservation. In contrast, when maintaining indoor temperature is given higher importance, the controller puts more effort into keeping optimal comfort levels instead of simply maximizing energy savings.

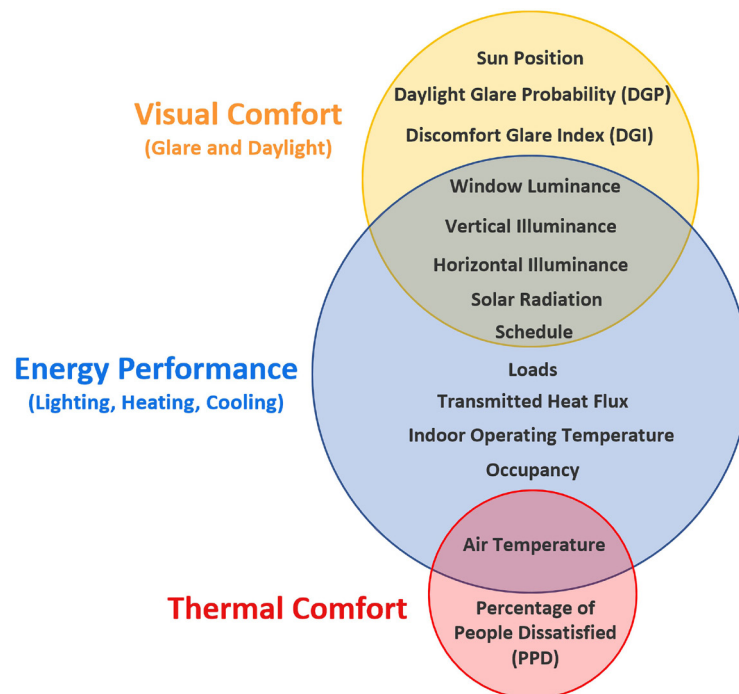


FIG. 8 Schematic representation of the main performance parameters, sensors and variables involved in optimizing energy and comfort conditions within a built environment.

Fig. 8 comprehensively illustrates the variables involved in optimising energy and comfort performances within a built environment. For instance, in terms of visual comfort, the MPC considers several factors such as the sun's position, Daylight Glare Probability (DGP), Discomfort Glare Index (DGI), window luminance, and solar radiation. It also takes into account changes over time, such as the shifting position of the sun and seasonal variations in daylight availability.

Thermal comfort is another crucial aspect, with key indicators like the temperature of the inner glass surface and the Percentage of People Dissatisfied (PPD). These factors demand a sophisticated understanding of the building's thermal characteristics and the ability to anticipate and respond to changes in the external environment and occupant behaviour.

For energy performance, a wide range of variables are considered, such as window luminance, solar radiation, transmitted heat flux, loads, indoor operating temperature, occupancy, and air temperature. The MPC must be designed to adapt dynamically to changing conditions and demands to optimise the energy efficiency of the building.

The possibility to adjust light and heat transmittance independently allows for a greater degree of control in balancing the multiple dimensions of building performance. This feature aligns seamlessly with an MPC's ability to dynamically adapt and manage a wide range of variables. The synergy between PLSMC technology and an advanced MPC system can definitively provide a uniquely adaptable solution to the multidimensional challenge of optimizing building performances.

While advanced control strategies like Rule-Based Control harness the potential of dynamic glazing systems, the research presented in Section 4 delves deeper into the optical and thermal features of the PLSMC and the implications for building performance.

4 PERFORMANCE OUTCOMES AND DATA ANALYSIS

Emerging from the foundational research on plasmochromic materials, we now turn our attention to their practical application within Insulated Glazing Units. Their energy efficiency and potential to enhance occupant comfort are scrutinised, drawing direct comparisons with conventional glazing systems prevalent in sustainable building design.

4.1 OPTICAL AND THERMAL CHARACTERISATION OF PLSMC MODULES

The transmittance spectra of PLSMC modules at different optical states (corresponding to specific values of a bias voltage applied between the PLSMC electrode and counter electrode) are reported in Fig. 9c. The high transparency these modules showcase over the entire solar spectral range when in the initial bleached (OFF) state must be remarked. In this state, the solar transmittance (T_{sol}) and luminous transmittance (T_{LUM}) values register at an impressive 79% and 75%, respectively, revealing the module's substantial transmissive capabilities.

Upon applying moderate bias potentials, a progressive attenuation of the optical transmittance within the NIR region begins to emerge. This perceptible change evolves until it eventually culminates in a complete extinction of incident solar radiation within the range of 780 to 1600 nm (this corresponds to T_{NIR} values of less than 1%). This intriguing occurrence of NIR light shielding is contrastingly paired with a modest decline in visible transmittance, maintaining T_{LUM} values greater than 46% even for applied biases of less than -1.5 V.

However, as the voltages decrease further, there is a noticeable impact on T_{LUM} , which also begins to decline. This leads to the glass acquiring a characteristic deep blue hue. The emergence of this scattering phenomenon is intrinsically linked with the appearance of a powerful optical extinction band, which subsequently causes an increase in the reflectance within the NIR range. Pushing the bias to its maximum sustainable potential, approximately -2.7 V, results in a steep drop in T_{LUM} values to below 5%, which transpires around 15 minutes from the initial bleaching state.

This decrease in optical contrast is primarily driven by a blue shift of the absorption band, thereby causing a dominant blue tone. This is a characteristic property of significantly reduced tungsten oxide. However, its spectral response is not entirely aligned with the human eye's response (approximately 400 to 700 nm). This mismatch presents a considerable limitation for the luminous transmittance (TLUM) and, hence, inevitably affects the value of the ratio of luminous to solar transmittance (TLUM/TSOL).

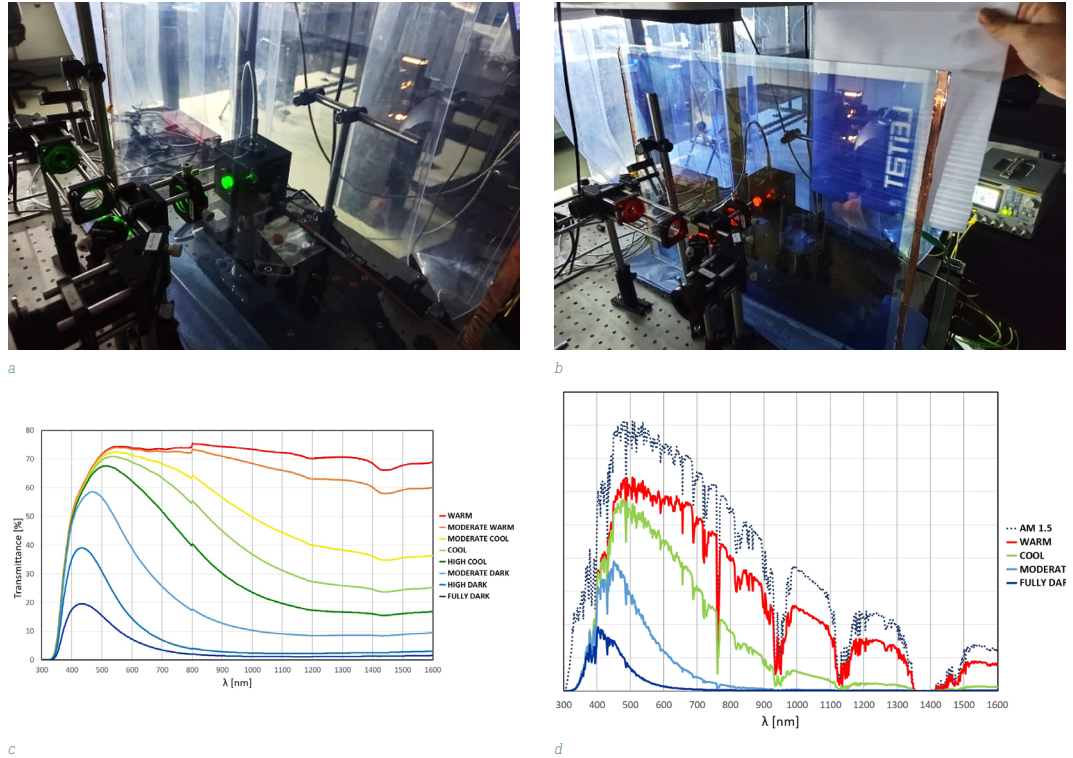


FIG. 9 a,b) The set-up adopted to measure the transmittance spectra of PLSMC modules. c) Transmittance spectra and d) solar irradiance spectra at different applied voltages to the PLSMC device.

The most meaningful features of the above presented PLSMC modules – namely the dynamic range of optical modulation both in the VIS (T_{LUM}) and NIR (T_{NIR}) – and the corresponding colouring and bleaching time (namely t_c and t_b) are summarised in TABLE 1.

TABLE 1 Main parameters and properties of a PLSMC module

INFINITE PLSMC modules	
PLSMC IGU size	Not integrated into IGU $3\% < T_{LUM} < 75\%$ (EN 410) $5\% < T_{NIR} < 79\%$ (EN 410)
Maximum Optical Modulation	$2\% < T_{SOL} < 79\%$ (EN 410)
Spectral Selectivity	T_{LUM}/T_{SOL} (in cool mode) > 1.5
Switching Speed	$t_{col}@600nm < 10 \text{ min}$ / $t_{bleach}@600nm < 15 \text{ min}$ $t_{col}@1500nm < 3 \text{ min}$ / $t_{bleach}@1500nm < 25 \text{ min}$
SHGC (dynamic range)	To be measured upon integration in IGU
Abs. Power Density	$< 300 \text{ mW/m}^2$
Electrochemical Stability	> 1000 colouring/bleaching cycles @ RT
Thermal Stability	> 500 cycles @ 85°C & 40% RH

To illustrate this effect, we conducted a comprehensive examination, presenting a semi-quantitative analysis of the reversible temperature modulation observed on the PLSMC glass surface, as well as on a black surface situated directly behind it, as depicted in Fig. 10. In this experimental series, a VarioCAM® HR InfraTec camera was employed to capture a series of infra-red images of the device under varying bias and exposure conditions. A representative depiction of the experimental setup is provided in Fig. 10. The IRBIS 2.2 software, supplied by InfraTec, was utilised for editing the acquired IR images.

The experiment involved a 12x12 cm² device, which was subjected to sunlight radiation via a solar simulator, with a light source casting a nominal intensity of one sun on an AM1.5 filter. The device then underwent exposure to the previously mentioned bias voltages. The observable outcomes reveal that, after an exposure period of 40 minutes at the OCP with $T_{LUM} = 75\%$ and $T_{SOL} = 79\%$, there is a notable increase in temperature on the top surface by approximately 7°C, changing from 26°C to 33°C. Simultaneously, the surface of the background black paper registered a temperature surpassing 40°C.

Following this, the experimental setup underwent a cooling process back to Room Temperature (RT), and the device was then shifted into a NIR-blocking state, with $T_{LUM} = 54\%$ and $T_{SOL} = 34\%$ at -1.5V. The temperature measurement procedure was then repeated, as seen in Fig. 10e-h. Under these conditions, the temperature recorded behind the glass did not rise above 38°C, while the top of the glass registered a temperature of 35°C.

At a lower bias potential, specifically at -2.7V, the black surface appeared almost completely protected by the PLSMC device in its fully absorbing state, with T_{SOL} dropping below 2%. The surface temperature of this black surface was only marginally higher than the surrounding unexposed environment, as illustrated in Fig. 10i-l. After a 40-minute exposure period at 1sun, the PLSMC device itself reached a temperature of 42°C.

In comparison with commercially available EC glazing, the devices presented in this study demonstrate considerable advantages, showcasing an expansive modulation of the overall solar radiation ($\Delta T_{SOL} = 77\%$). They exhibit high visible light transmission in the bleached state ($T_{LUM} = 75\%$ at OCP), coupled with strong optical contrast ($\Delta T_{LUM} = 72\%$ between OCP and -2.7 V). These parameters indicate a robust performance across various spectrums and voltage conditions. However, a unique distinction is worth noting. Typically, for EC devices, a reduction in T_{LUM} corresponds to a proportionate decrease in T_{NIR} , and consequently in T_{SOL} , across the entire control range. In contrast, PLSMC systems at low to moderate bias potentials provide the ability to substantially lower T_{SOL} by about 40% while still retaining a T_{LUM} value above 50%.

It is crucial to emphasise that these data should only be applied to carry out a meaningful quantitative analysis when considering the precise set of experimental conditions under which they were acquired. These conditions include specific characteristics of the light source (a 150 W xenon short arc lamp was used for this experiment), the distance between the lamp and the glass (approximately 15 cm in this case), the ventilation conditions, the emissivity of the thermocamera, and several other factors.

This unique attribute can be strategically exploited to optimise energy consumption in buildings and enhance both thermal and daylight comfort levels. For instance, in climates dominated by cooling requirements, the considerable reduction in solar thermal radiation entering the glazing can help decrease energy usage without significant compromise to the transparency of the glass.

This feature thus has the potential to mitigate overheating problems while minimally impacting daylight infiltration. Conversely, during the heating season or in climates primarily requiring heating, PLSMC devices can be adjusted to allow higher levels of solar energy transmission. This is achievable because a high T_{LUM} can be maintained, which can effectively offset a substantial portion of the building's heating energy requirements. As such, PLSMC devices serve as a versatile solution, catering to varying energy needs across diverse climatic conditions.

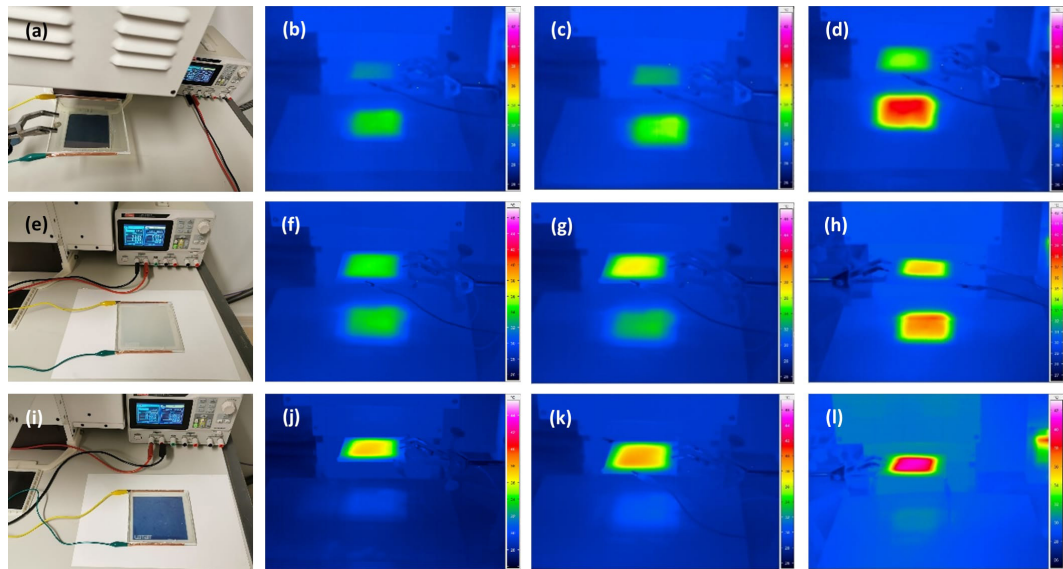


FIG. 10 Thermo-camera pictures of a PLSMC device exposed to sunlight radiation. (a) Initial picture of the setup before turning on the solar simulator; (c-d) changes observed until reaching 40 min of solar irradiation. (e) Picture of the device after 40 min at an applied potential of -1.5V and the corresponding IR-images (f-h) during 40 min of continuous illumination. Finally, (i) picture taken at -2.7V after 40 min under solar light exposure and (j-l) its IR-images (Cots, et al., 2021).

Nevertheless, to comply with the requirements of some extreme building façade operative conditions (Poláková, Schäfer, & Elstner, 2018), a marketable EC technology should guarantee adequate thermal and electrochemical stability. PLSMC modules have been tested in a CTS climatic chamber (Mod. CL-30/1000-BF+) by running a series of colouring/bleaching cycles at 85°C. The I-t curve (collected by an SP-150 Potentiostat/Galvanostat) is shown in Fig. 11b. The data reveal that no significant reduction in the galvanostatic current occurred over the first 500 cycles, as attested by the WARM and DARK transmittance spectra measured (again) upon the thermal ageing test.

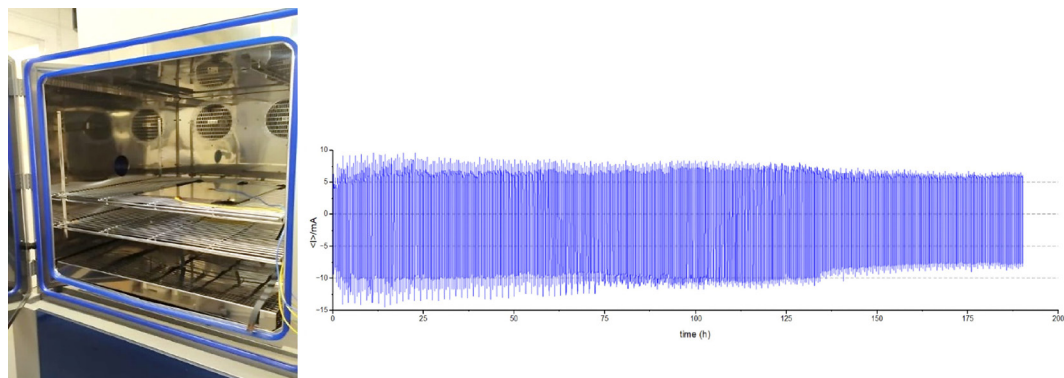


FIG. 11 (a) Climatic chamber used for the thermal ageing test of the PLSMC devices. (b) Variation of the electric current measured over 200 hours (about 500 cycles) under cycling a 45x55cm² PLSMC device at 85°C and 40% RH.

A good compromise between EC performance and environmental stability can be claimed. However, it is pertinent to note that achieving this balance will necessitate additional industry-driven design optimisation efforts. These efforts will be crucial in ensuring that the PLSMC modules adhere to both technical standards and international norms.

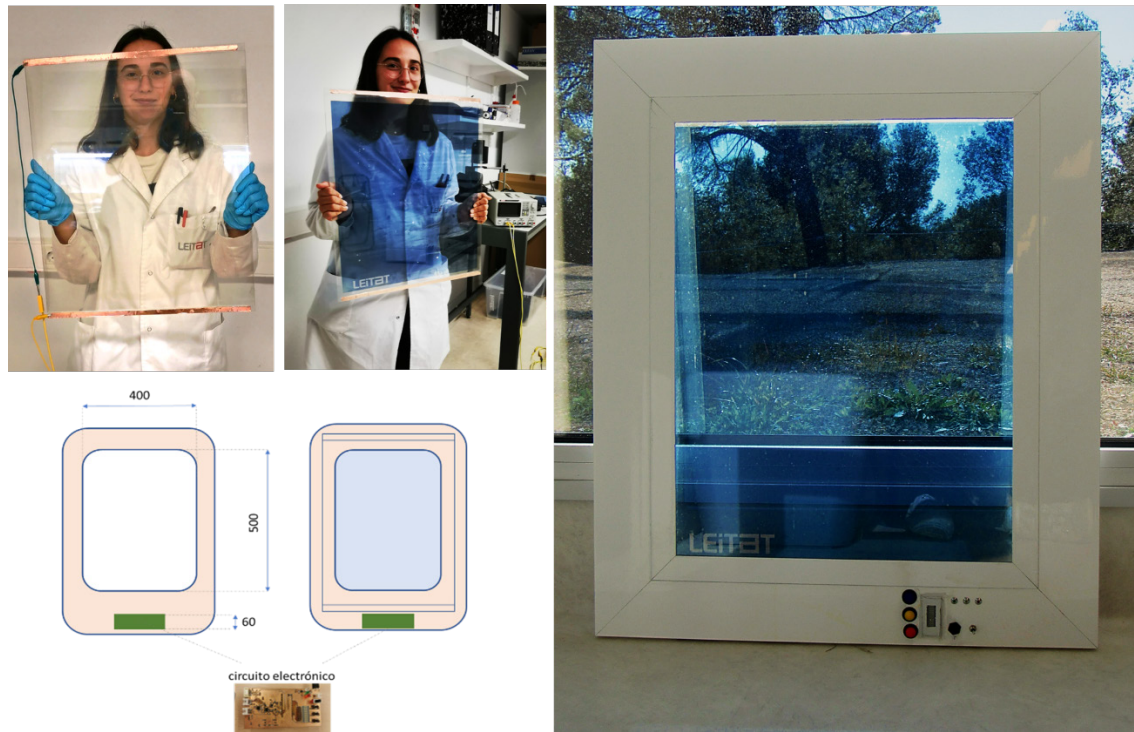


FIG. 12 (a), (b) and (c) are photos of the 45x50 cm² PLSMC prototype module realized in the frame of the INFINITE project. (d) Represent a schematic drawing of the demonstrator embedding an ad-hoc implemented control circuit.

While the experimental observations demonstrate the capabilities of the PLSMC devices, Section 4.2 delves deeper into the design and benchmarking of an efficient PLSMC IGU, highlighting its potential advantages in building envelopes compared to commercial alternatives.

4.2 DESIGN OF AN EFFICIENT PLSMC IGU AND COMPARISON WITH BENCHMARK TECHNOLOGIES

The energy-saving potential of PLSMC modules can be fully exploited in a building envelope only if they are integrated into a well-designed IGU, which must also account for a low thermal transmittance (U-value), typically within the range of 1.0 to 1.4 W/m²K for a well-designed DGU. To this purpose, the appropriate choice of glass panes, interlayer coatings, and cavity gas is of crucial importance. In particular, the proper choice of a low-E coating permits increasing the modulation range of the g-value and maximises the peculiar benefits of the PLSMC system in terms of energy saving and visual/thermal comfort.

As mentioned before in paragraph 2.2 and represented in Fig. 5, the PLSMC DGU considered and modelled in this article presents a layer structure made of clear float glass, a PVB interlayer, the PLSMC device, a 16 mm air gap with a gas mixture made of 90% Argon and 10% air, and a Low-E clear float glass ($\epsilon = 0.04$).

The KPIs of this DGU have been compared with those of three benchmark DGUs chosen based on their common usage in contemporary architecture and their distinctive features.

The first benchmark is an EC DGU made with commercial EC glass, specifically SageGlass Classic SR2.0, and it has an internal low-E coating ($\epsilon = 0.04$) that reduces the amount of UV and IR light that can pass through the glass without compromising the amount of visible light transmission. This combination of EC technology and low-E coating allows for dynamic control of light and heat transmission.

The second benchmark is a DGU with an internal low-E coating and an external blind, specifically the Hella AR92S blind. This system represents a more traditional approach to managing solar heat gain and light transmission, combining the energy-efficient properties of low-E glass with the flexibility of external blinds.

Finally, the third benchmark is a triple glazing unit (TGU) with an internal low-E coating and internal blinds, specifically the Pellini V95. Triple glazing offers superior thermal insulation compared to double glazing, making it a popular choice for high-performance buildings in colder climates. Pellini V95 blinds are integrated into the window system, allowing for seamless control of light and privacy without affecting the window's thermal performance.

By comparing the performance of the PLSMC-based DGU with these benchmarks, the study aimed to understand how this novel technology stacks up against existing solutions in terms of thermal comfort, visual comfort, and energy efficiency. TABLE 2 summarises the most meaningful characteristics of the selected benchmarks together with one of the PLSMC DGU.

TABLE 2 Thermal and optical features of the PLSMC DGU and of three commercial glazing systems

IGU	STATE	U-value	g-value	T _{LUM}	T _{SOL}
		[W/m ² K]			
PLSMC (DGU) Clear float Glass 6mm / PVB/ PLSMC device/16mm 90% Argon, 10% Air/ Low-E clear float glass 6mm	WARM	1.2	0.64	0.73	0.52
	MODERATE WARM		0.54	0.71	0.45
	MODERATE COOL		0.40	0.64	0.31
	COOL		0.32	0.56	0.23
	HIGH COOL		0.24	0.43	0.16
	MODERATE DARK		0.17	0.28	0.11
	HIGH DARK		0.12	0.17	0.09
	FULLY DARK		0.07	0.03	0.02
SAGEGLASS EC (DGU) SageGlass SR2.0 9mm/ 16mm 90% Argon, 10% Air/ Low-E clear float glass 6mm	BLEACHED	1.2	0.40	0.57	0.33
	TINTED 1		0.22	0.34	0.16
	TINTED 2		0.14	0.20	0.08
	TINTED 3		0.09	0.05	0.02
	FULLY TINTED		0.08	0.01	0.05
HELLA AR92S (DGU) Hella AR92S/ Clear float glass/ 16mm 90% Argon, 10% Air/ Low-E clear float glass 6mm	TILT 0 °	1.2	0.63	0.73	0.52
	TILT 55 °		0.08	0.06	0.04
	TILT 90 °		0.02	0.00	0.00
PELLINI V95 (TGU) Clear float glass 6mm/ Pellini V95/ Clear float glass 6mm/ 14mm 90% Argon, 10% Air/ Low-E clear float glass 6mm	TILT 0 °	0.7	0.53	0.68	0.45
	TILT 55 °		0.17	0.18	0.04
	TILT 90 °		0.02	0.00	0.00

The data detailed in the table has been subjected to a thorough analysis; Fig. 13 presents the results in a plot of g-value versus T_{LUM} . This approach to data representation facilitates a more intuitive comparison of the various technologies under consideration. The g-value vs T_{LUM} plot serves as a tool to provide a visual representation of how each technology allows for the transmission of light (T_{LUM}) and heat (g-value), which are both critical factors in determining the overall performance of a window system. The horizontal axis of the plot represents the g-value, an important measure of a window's ability to transmit solar energy and, hence, contribute to the heating of a space. The vertical axis, on the other hand, represents T_{LUM} , the percentage of visible light that passes through a window system.

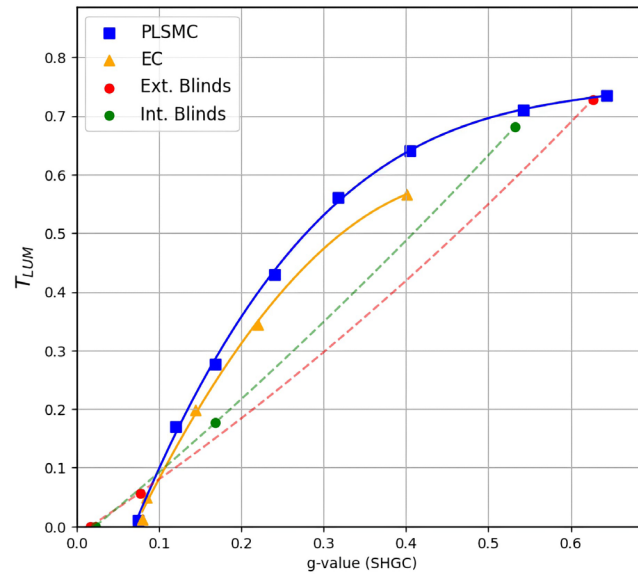


FIG. 13 T_{LUM} vs g-factor (SHGC) curves for the glazing and shading technologies considered.

These data reveal that the integration of PLSMC technology into a correctly designed IGU may turn in the considerable improvements over some of the existing advanced shading systems taken as benchmarks shown in TABLE 3:

TABLE 3 Characteristics and benefits of PLSMC DGUs in comparison to the selected benchmarks

Features/Advantages	Description
Wide Modulation Capability	PLSMC DGUs have a Δg of 0.57, with over 0.30 in visible transmission above $T_{LUM} > 60\%$, reducing solar loads and balancing cooling with daylight. In cold climates, the wide Δg enhances solar heat on sunny days.
Optical Contrast in VIS Range	PLSMC DGU's T_{LUM} ranges from 0.73 to 0.03, ensuring ample daylight in buildings with a low g-value and options down to 3% T_{LUM} for visual comfort.
Flexibility Over Benchmarks	Compared to Pellini internal blinds and Hella external blinds, PLSMC boasts greater flexibility, offering precise control over light modulation and dynamic adjustment of light transmittance and g-value.
Overall Benefits of PLSMC DGU	The technology enhances g-value modulation and solar gain across climates, impacting energy and thermal comfort. Its luminous transmittance is on par with blind benchmarks, ensuring better visual comfort.

To summarise, the advantages of the PLSMC DGU with respect to the chosen benchmarks are a wider modulation capability of the g-value, which improves the possibility of using this glazing as a solar gain modulator, useful both in heating and cooling-dominated climates and with a direct effect on energy needs and thermal comfort; a large luminous transmittance range, even comparable to the benchmarks with blinds, which ultimately allows the PLSMC DGU to guarantee better levels of visual comfort. Moreover, the peculiar shape in the T_{LUM} -g plot suggests an interesting potential in managing high g-values while not compromising T_{LUM} (useful in heating periods, where solar gains are a plus and the possibility of maintaining high transmittances is appreciated for visual purposes).

5 CONCLUSIONS & PERSPECTIVES

We have been working on the development of EC glazing with extended control functionalities in the NIR region. In this paper, we presented the most recent achievements and prospected their competitive advantages with respect to analogous commercial solutions. IGUs integrating PLSMC technology have indeed great potential in terms of the capability to modulate solar loads and visible light beyond what is currently achievable with full solid-state EC devices. They ultimately impact the total building energy use (lighting, cooling, and heating) and the occupant comfort (visual comfort, in terms of daylight availability and perceived glare discomfort, and thermal comfort).

Future efforts will focus on enhancing PLSMC materials and module design. Spectral selectivity can be improved using alternative electro-active materials that align with the photopic human eye normalisation spectrum. The visible blue appearance in the "DARK state" can be adjusted for better colour neutrality. The next steps will assess this potential and aim to optimise control, reducing building energy use, and occupant discomfort. Separating the NIR and VIS ranges facilitates superior control strategies, a concept unexplored thus far. Past adaptive glazing system designs balanced thermal and visual domains. This separation invites new control strategies that consider these aspects independently, simplifying the controller and improving indoor environment influence. The insights derived from this process were not only informative but also invaluable for shaping the future trajectory of PLSMC technology in the field of modern building design.

Acknowledgements

This publication was funded by the European Union from the European Union's Horizon Europe Research and Innovation Programme under Grant Agreement No 958397, INFINITE. Views and opinions expressed are however those of the author(s) only and do not necessarily reflect those of the European Union. Neither the European Union nor the granting authority can be held responsible for them.

This work was partially supported by the Spanish Ministry for Science and Innovation (MICINN) through the "Ramon y Cajal" grant awarded to Dr. Michele Manca (ref. RYC2018-024399-I).

References

- Barawi, M., Veramonti, G., Epifani, M., Giannuzzi, R., Sibillano, T., Giannini, C., . . . Manca, M. (2018). A dual band electrochromic device switchable across four distinct optical modes. *Journal of Materials Chemistry A*, 6, 10201–10205. Retrieved from <https://doi.org/10.1039/C8TA02636J>
- Cao, S., Zhang, S., Zhang, T., & Lee, J. Y. (2018). Fluoride-Assisted Synthesis of Plasmonic Colloidal Ta-Doped TiO₂ Nanocrystals for Near-Infrared and Visible-Light Selective Electrochromic Modulation. *Chemistry of Materials*, 30, 4838–4846. Retrieved from <https://doi.org/10.1021/acs.chemmater.8b02196>
- Cao, X., Dai, X., & Liu, J. (2016). Building energy-consumption status worldwide and the state-of-the art technologies for zero-energy buildings during the past decade. *Energy and Buildings*, 128, 198–213. Retrieved from <https://doi.org/10.1016/j.enbuild.2016.06.089>
- Cots, A., Dicorato, S., Giovannini, L., Favoino, F., & Manca, M. (2021). Energy Efficient Smart Plasmochromic Windows: Properties, Manufacturing and Integration in Insulating Glazing. *Nano Energy*, 84, 105894. Retrieved from <https://doi.org/10.1016/j.nanoen.2021.105894>
- Danza, L., Barozzi, B., Bellazzi, A., Belussi, L., Devitofrancesco, A., Ghellere, M., . . . Scrosati, C. (2020). A weighting procedure to analyse the Indoor Environmental Quality of a Zero-Energy Building. *Building and Environment*, 107155. Retrieved from <https://doi.org/10.1016/j.buildenv.2020.107155>
- Favoino, F., & Overend, M. (2015). A Simulation Framework for the Evaluation of Next Generation Responsive Building Envelope Technologies. *Energy Procedia*, 78, 2602–2607. Retrieved from <https://doi.org/10.1016/j.egypro.2015.11.302>
- Garcia, G., Buonsanti, R., Runnerstrom, E. L., Mendelsberg, R. J., Llordes, A., Anders, A., . . . Milliron, D. J. (2011). Dynamically Modulating the Surface Plasmon Resonance of Doped Semiconductor Nanocrystals. *Nano Letters*, 11, 4415–4420. Retrieved from <https://doi.org/10.1021/nl202597n>
- Giannuzzi, R., Scarfiello, R., Sibillano, T., Nobile, C., Grillo, V., Giannini, C., . . . Manca, M. (2017). From capacitance-controlled to diffusion-controlled electrochromism in one-dimensional shape-tailored tungsten oxide nanocrystals. *Nano Energy*, 41, 634–645. Retrieved from <https://doi.org/10.1016/j.nanoen.2017.09.058>
- Giovannini, L., Favoino, F., Pellegrino, A., Lo Verso, V. R., Serra, V., & Zinzi, M. (2019). Thermo-chromic glazing performance: From component experimental characterisation to whole building performance evaluation. *Applied Energy*, 251, 113335. Retrieved from <https://doi.org/10.1016/j.apenergy.2019.113335>
- Isaia, F., Fiorentini, M., Serra, V., & Capozzoli, A. (2021). Enhancing energy efficiency and comfort in buildings through model predictive control for dynamic façades with electrochromic glazing. *Journal of Building Engineering*, 43, 102535. Retrieved from <https://doi.org/10.1016/j.jobe.2021.102535>
- Li, S. Y., Niklasson, G. A., & Granqvist, C. G. (2012). Plasmon-induced near-infrared electrochromism based on transparent conducting nanoparticles: Approximate performance limits. *Applied Physics Letters*, 101, 07190. Retrieved from <https://doi.org/10.1063/1.4739792>
- Manthiram, K., & Alivisatos, A. P. (2012). Tunable Localized Surface Plasmon Resonances in Tungsten Oxide Nanocrystals. *Journal of the American Chemical Society*, 134, 3995–3998. Retrieved from <https://doi.org/10.1021/ja211363w>
- Optics. (n.d.). Retrieved from Windows and Daylighting: <https://windows.lbl.gov/software/optics>
- Pallonetto, F., De Rosa, M., D’Ettorre, F., & P. Finn, D. (2020). On the assessment and control optimisation of demand response programs in residential buildings. *Renewable and Sustainable Energy Reviews*, 109861. Retrieved from <https://doi.org/10.1016/j.rser.2020.109861>
- Poláková, M., Schäfer, S., & Elstner, M. (2018). Thermal Glass Stress Analysis – Design Considerations. *Challenging Glass Conference Proceedings*, 6, 725–740. Retrieved from <https://doi.org/10.7480/cgc.6.2193>
- Roberts, J. A., De Michele, G., Pernigotto, G., Gasparella, A., & Avesani, S. (2022). Impact of active façade control parameters and sensor network complexity on comfort and efficiency: A residential Italian case-study. *Energy and Buildings*, 255, 111650. Retrieved from <https://doi.org/10.1016/j.enbuild.2021.111650>
- Standardization, E. C. (1998). *ISO EN 410:1998. Glass in building. Determination of luminous and solar characteristics of glazing*. Brussels.

- Standardization, E. C. (2011). *ISO EN 673:1997. Glass in building. Determination of thermal transmittance (U value)- Calculation method*. Brussels.
- Tsuboi, A., Nakamura, K., & Kobayashi, N. (2016). Chromatic control of multicolor electrochromic device with localized surface plasmon resonance of silver nanoparticles by voltage-step method. *Solar Energy Materials and Solar Cells*, 145, 16-25. Retrieved from <https://doi.org/10.1016/j.solmat.2015.07.034>
- WINDOW. (n.d.). Retrieved from Windows and Daylighting: <https://windows.lbl.gov/software/window>
- Xu, J., Zhang, Y., Zhai, T.-T., Kuang, Z., Li, J., Wang, Y., . . . Xia, X.-H. (2018). Electrochromic-Tuned Plasmonics for Photothermal Sterile Window. *ACS Nano*, 12, 6895–6903. Retrieved from <https://doi.org/10.1021/acsnano.8b02292>